JOURNAL OF MATERIALS SCIENCE 36 (2001) 1833–1841

The formation of α-Al_2O_3 from θ-Al_2O_3: The relevance of a "critical size" and: Diffusional nucleation or "synchro-shear"?

R. B. BAGWELL, G. L. MESSING, P. R. HOWELL
Department of Materials Science and Engineering, The Pennsylvania State University, University Park, PA 16802, USA
E-mail: messing@mrl.psu.edu

The coarsening of θ-Al_2O_3 crystals to a 'critical size' is often interpreted as the first step in the shear nucleation of α-Al_2O_3. The existence of this so-called critical size has also been used to explain the observation that α-Al_2O_3 "nuclei" are generally twice as large as the crystals in the θ-Al_2O_3 matrix. This paper discusses the important issues in the nucleation of α-Al_2O_3 from θ-Al_2O_3. A few key experiments are also presented to clarify the nucleation process. It is concluded that a critical θ-Al_2O_3 crystal size is not a prerequisite for α-Al_2O_3 nucleation, but is primarily a result of the incubation time required to produce α-Al_2O_3 nuclei by diffusional nucleation. It is proposed that the large observed α-Al_2O_3 crystal size also does not result from a shear nucleation event in a 'critical size' θ-Al_2O_3 crystal, but is due to the intrinsically low α-Al_2O_3 nucleation density, together with rapid growth of α-Al_2O_3 after nucleation. *© 2001 Kluwer Academic Publishers*

1. Introduction

1.1. Transformation to α-Al_2O_3

The properties of α-Al_2O_3 ceramics depend on the ability to control microstructural development and to obtain grain sizes $<1\ \mu$m at full density [1, 2]. Most α-Al_2O_3 precursors, such as bayerite (α-$Al(OH)_3$) and boehmite (γ-AlOOH), require calcination at $>500°$C and result in a series of transition aluminas before formation of α-Al_2O_3 [3–6]. The transition alumina crystal structures consist of cubic close packed (ccp) oxygen atoms with aluminum atoms in tetrahedral and octahedral interstices in a distribution largely determined by the temperature of calcination [4]. Transformations between transition aluminas are topotactic and therefore of relatively low energy [3–6]. The formation of θ-Al_2O_3, the most crystallographically ordered transition alumina, is often the final step before the transformation to α-Al_2O_3, particularly in boehmite-derived alumina [3–6]. The transformation from θ-Al_2O_3 to α-Al_2O_3 involves a change in the oxygen sublattice from cubic to hexagonal close packing (ccp $\rightarrow$ hcp) and generally occurs above $\sim$1200°C [3–6]. The transformation from θ-Al_2O_3 to α-Al_2O_3 is the critical step in controlling microstructural evolution for ceramic applications because of the significant changes in crystal size, density, pore size and pore size distribution [3–16]. Although the α-Al_2O_3 transformation has been reported to occur by diffusional nucleation and growth [5–16], the α-Al_2O_3 nucleation mechanism within single θ-Al_2O_3 crystals is not well understood because of the inability to directly observe the nm-scale nucleation event and the rapid growth of α-Al_2O_3 after nucleation.

The concept of a 'critical' θ-Al_2O_3 crystal size has been proposed as a key requirement for nucleation of α-Al_2O_3 [5, 7, 8, 17–28]. This proposal stems from the observation that θ-Al_2O_3 appears to coarsen significantly before α-Al_2O_3 forms. For example, Fig. 1a shows that pseudoboehmite-derived θ-Al_2O_3 crystals coarsen from $\sim$5 nm to $\sim$20 nm before the formation of α-Al_2O_3. The θ-Al_2O_3 never develops sharp, well defined XRD peaks. The α-Al_2O_3 crystals formed initially are nearly always considerably larger than this so-called critical size, as shown in Fig. 1b and produce XRD peaks with only a small degree of line broadening. Table I summarizes the "critical crystal sizes" of transition aluminas reported in the literature for a variety of alumina precursors and different heating conditions. The critical θ-Al_2O_3 crystal size and the much larger α-Al_2O_3 crystal size are important phenomenological concepts in controlling the transformation to α-Al_2O_3. The final α-Al_2O_3 grain size, for instance, is dependent on controlling the initial α-Al_2O_3 crystal size and the nucleation density. On the other hand, if the goal is to retain the high surface area transition alumina, increasing the critical size and thereby inhibiting the α-Al_2O_3 transformation would be beneficial. Likewise, if high surface area α-Al_2O_3 is desired then information about how to form α-Al_2O_3 from transition aluminas prior to coarsening would be useful.

1.2. Shear nucleation

Two mechanisms have been proposed for the nucleation of α-Al_2O_3 from θ-Al_2O_3; shear nucleation and

0022–2461 *© 2001 Kluwer Academic Publishers*

TABLE I Critical crystal size effects reported in previous studies

Critical crystal size	Initial α nuclei size	Precursor	Heating cond.	Reference
'Small'	500–1000 nm	Boehmite	1000–1100°C	5
50 nm	1000 nm	Alum-derived	1150	7
20 nm*	—	Doped γ-Al_2O_3	995–1100	8
31 nm*	—	Boehmite	1100–1225	11
13 nm*	—	Transition Al_2O_3	high T H_2O	17
—	150 nm	Transition Al_2O_3	high T H_2O	18
—	50 nm	Sulfate derived	1150–1200	19
10 nm	100 nm	Alum derived	1100–1200	20
13 nm	90 nm	Doped boehmite	1200	21
22 nm*	—	HF mineralized	800–1200	22
20 nm	70 nm	Boehmite	750–1400	23
30 nm	40 nm	Organic	1050	24
60 nm	100 nm	Bayerite	1080–1180	25
50 nm	—	γ-Al_2O_3 films	1200	26
20–30 nm	100 nm	Al_2O_3 compacts	600–1320	27
20 nm	'no line broadening'	Hydroxides	950–1050	28

*Calculated from surface area data.

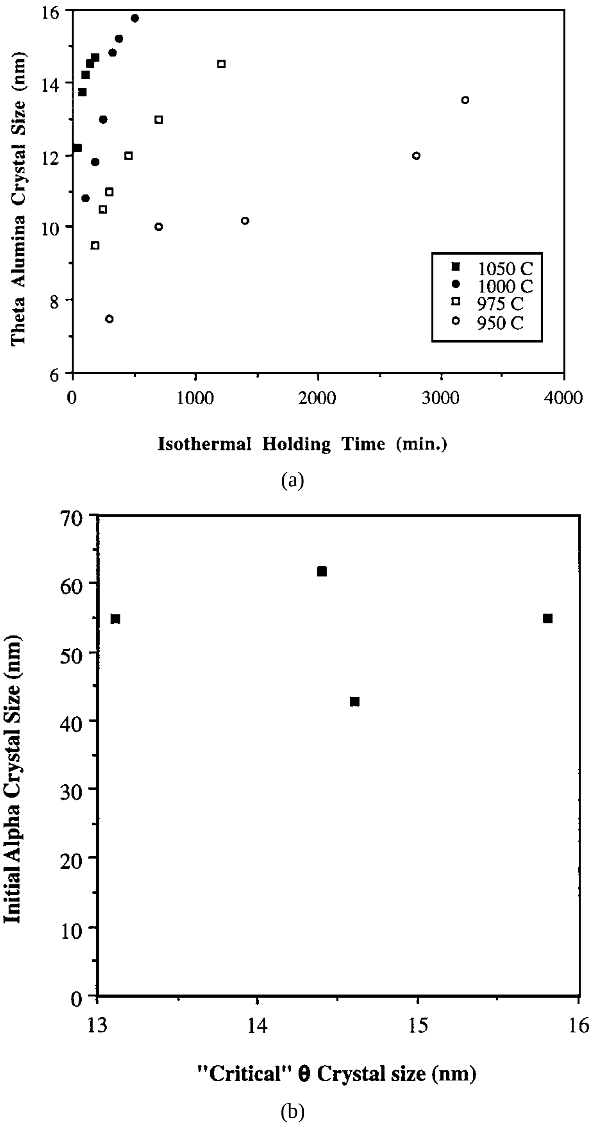

(a)

(b)

Figure 1 (a) Coarsening of θ-Al_2O_3 crystals to the so-called 'critical size' before the nucleation of larger α-Al_2O_3 crystals. (b) Initial α-Al_2O_3 crystal size plotted against final θ-Al_2O_3 crystal size.

diffusional nucleation. Shear, or martensitic, transformations are diffusionless and may propagate through crystals at velocities approaching the speed of sound [29–33]. In a shear process all of the atoms in a volume of the transforming matrix simultaneously shift a short distance into the new structure. For example, a cubic close packed metal structure such as cobalt can be converted into a hexagonal close packed structure by the motion of $a/6\ \langle 121\rangle$ Shockley partial dislocations over alternate close packed planes [29, 30]. The shift of the various lattice planes frequently results in a large concentration of stacking faults that can be easily observed by transmission electron microscopy (TEM) [29, 30].

The apparent dependence of the nucleation of α-Al_2O_3 on the crystal size of the θ-Al_2O_3 led to the application of the shear nucleation model to the transformation. Shear transformations commonly encounter grain and crystal size effects due to the cooperative nature of the atomic movements involved [29]. Surfaces, grain boundaries, and defects contain atoms that are not as constrained as an atom in the bulk of the crystal and thus resist a cooperative transformation process. Small crystals contain a greater number of surface atoms per unit volume than larger crystals and are therefore less likely to transform martensitically [29]. Smaller crystals also contain fewer potential nucleating defects which decreases the chance of catalyzing the nucleation process [29, 30]. It has been proposed that θ-Al_2O_3 coarsens until the largest θ-Al_2O_3 crystals reach a size where they can shear to form α-Al_2O_3. The larger average α-Al_2O_3 crystal size is then said to develop because the α-Al_2O_3 nucleates in and consumes only the largest θ-Al_2O_3 crystals, as illustrated schematically in Fig. 2a. One point that should be emphasized is that the shear nucleation theory only addresses the nucleation mechanism. Growth of α-Al_2O_3 must proceed by a diffusional growth process that leads to the vermicular microstructure characteristic of α-Al_2O_3 formed from a transition alumina [7, 10, 11, 13, 16]. The question may then be raised. If growth is diffusional (by definition, the reaction is massive), then why would nucleation involve shear?

1.3. Diffusional nucleation

Diffusional nucleation is the more classical thermodynamic explanation for the formation of a new phase within a matrix. The energy barrier for diffusional

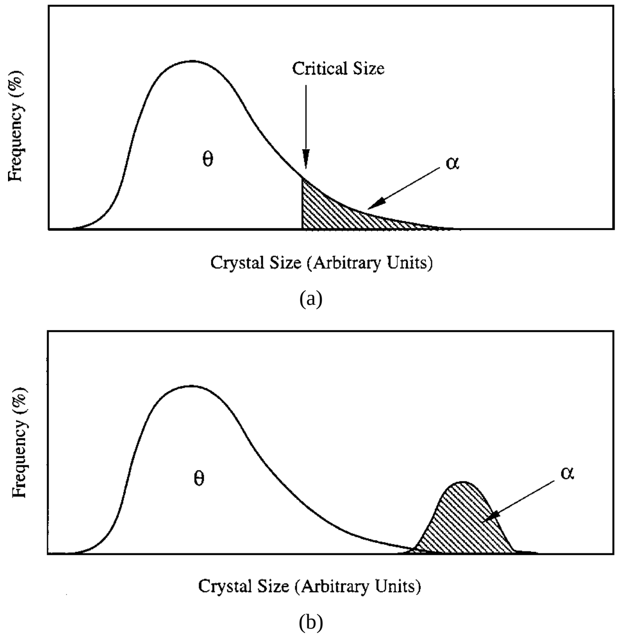

Figure 2 Schematic diagrams of the relationship between the θ-Al_2O_3 particle size and the α-Al_2O_3 particle size. (a) Conversion of "super-critical" θ crystallites to α by "shear". (b) development of a bi-modal size distribution due to diffusional nucleation followed by rapid growth of α from θ.

nucleation arises from e.g., the creation of a new surface between the nucleating (α) and matrix (θ) phase. A thermodynamically unstable embryo first forms and atoms attach and detach depending on statistical fluctuations [30]. The free energy barrier for heterogeneous nucleation on a substrate or grain boundary is much lower than for homogeneous nucleation, especially if the heterogeneity and nucleating phase have similar crystal structures [30]. Since diffusional nucleation is more favorable at surfaces and boundaries, α-Al_2O_3 would be expected to nucleate at the surface of θ-Al_2O_3 crystals or at necks between crystals. A 'critical' crystal size might be necessary for diffusional nucleation because the θ-Al_2O_3 crystals must coarsen to a sufficient degree to produce potent heterogeneous α-Al_2O_3 nucleation sites. Diffusionally nucleated α-Al_2O_3 crystals could still be larger than the crystals in the θ-Al_2O_3 matrix due to rapid growth of the α-Al_2O_3 after nucleation, in addition to nucleation occurring in the larger θ-Al_2O_3 crystals. Note that the rapid formation of large (massive) α-Al_2O_3 crystals is also favored by the exothermicity of the θ-Al_2O_3 to α-Al_2O_3 transformation. In this latter case, the distribution of α crystal sizes would be similar to that shown in Fig. 2b.

The focus of the present work is to critically review the issues involved in the nucleation of α-Al_2O_3 from θ-Al_2O_3, with an emphasis on the importance of the critical crystal size. The evidence for both shear and diffusional nucleation is presented along with supporting experiments from the literature and this investigation. Boehmite is used as a model for the behavior of alumina precursors which transform to α-Al_2O_3 via transition aluminas because it is available in two different crystal sizes; well-crystallized boehmite (>50 nm) and pseudoboehmite (~5 nm), which facilitates study of the nucleation process.

2. Discussion of nucleation mechanism

2.1. Evidence for shear nucleation

Kachi *et al.* [34] proposed a shear nucleation mechanism for the transformation of γ-Fe_2O_3 to α-Fe_2O_3 based on electron diffraction patterns of γ-Fe_2O_3 single crystals. They developed the 'synchro-shear' model after analyzing the orientation relationship;

$$(111)\gamma//(0001)\alpha$$
$$[1\bar{1}0]\gamma//[01\bar{1}0]\alpha$$

in transforming crystals. The authors proposed that shear of the oxygen lattice in the $\langle 112 \rangle$ direction, accompanied by a systematic shift of the Fe^{3+} ions, converts the fcc γ-Fe_2O_3 structure to hcp α-Fe_2O_3. However, it should be appreciated that the observation of an orientation relationship by itself is not unambiguous evidence for a shear transformation [41] because orientation relationships are virtually ubiquitous during diffusional nucleation and growth transformations. In addition, Kachi *et al.*, [34] did not identify e.g., an invariant plane.

The 'synchro-shear' model was first applied to the γ-Al_2O_3 to α-Al_2O_3 transformation by Bye and Simpkin [8], based on the apparent dependence of α-Al_2O_3 nucleation on the θ-Al_2O_3 crystal size and the crystallographic similarity of the γ to α-Fe_2O_3 and γ to α-Al_2O_3 transformations. They studied the transformation of pure, Fe-, and Cr-doped γ-Al_2O_3 to α-Al_2O_3 and found that Fe enhanced the transformation while Cr inhibited it. They measured the surface area as a function of the fraction of transition alumina transformed to α-Al_2O_3. The γ-Al_2O_3 coarsened from ~260 m^2/g to ~90 m^2/g before the transformation to α-Al_2O_3 began. The authors proposed that the θ-Al_2O_3 crystals 'sintered' to a critical size, and then a 'cluster' transformed to α-Al_2O_3 by shear displacement of the oxygen layers.

Wynnyckyj and Morris [25] reported a synchro-shear model for α-Al_2O_3 formed in bayerite (α-$Al(OH)_3$) gels. They determined a maximum θ-Al_2O_3 crystallite size of ~60 nm and a minimum α-Al_2O_3 crystal size of ~100 nm using x-ray line broadening. They used a statistical distribution model to explain their transformation data. The model assumed a Gaussian distribution of θ-Al_2O_3 crystal sizes with a mean size that increased with time when the θ-Al_2O_3 was heated. In their model a θ-Al_2O_3 crystal transforms to α-Al_2O_3 when the θ-Al_2O_3 reaches a critical size. The percent conversion to α-Al_2O_3 was related to a Z parameter in a probability-integral table. The values of Z were plotted as a function of the square root of time. The data fit the model very well, but the authors admit that some of the success may be due to the simplications in the analysis. In addition, the Z parameter is proportional to an appropriate diffusivity and:

$$Z = k'\sqrt{\mathrm{Dt}} + C \tag{1}$$

where k' and C are constants and $\sqrt{\mathrm{Dt}}$ is a characteristic diffusion length. Wynnyckyj and Morris also claimed that the application of the Avrami analysis to the $\theta \rightarrow \alpha$ transformation was questionable because "... the crystallite size of the theta should decrease while that of the alpha increases." The authors then stated that "There is no evidence of decrease of crystallite size of the precursor phase, theta, during the transformation." However, the major assumptions of the Avrami analysis involve the nucleation/growth rates of the product phase (i.e., the α-Al_2O_3) together with the spatial distribution of the product. The size of the parent phase (theta) is not relevant.

Hayashi *et al.* [24] studied the critical size evolution and transformation of θ-Al_2O_3 to α-Al_2O_3 using TEM and XRD. The θ-Al_2O_3 and α-Al_2O_3 crystal size distributions only overlapped at the upper end of the θ-Al_2O_3 distribution and the lower end of the α-Al_2O_3 distribution. The average θ-Al_2O_3 crystal size was never larger than ~30 nm while the average α-Al_2O_3 crystal size was never smaller than ~40 nm, leading the authors to support the synchro-shear mechanism. However, as noted earlier, diffusional nucleation followed by rapid, massive growth of the α-Al_2O_3 will yield different size populations for the α and θ phases (Fig. 2b). Hayashi *et al.* [24] also proposed a more complex crystallographic model of the transformation involving sliding of the oxygen layers along the $[1\bar{9}2]$ direction.

Chou and Nieh [26] considered a shear nucleation model for sputtered thin films of alumina. The authors reported the following orientation relationship:

$$(001)\gamma//(0001)\alpha$$
$$[4\bar{4}0]\gamma//[\bar{3}030]\alpha$$
$$[3\bar{1}0]\gamma//[\bar{2}110]\alpha$$

between the γ-Al_2O_3 matrix and α-Al_2O_3 nuclei during the transformation. Based on their observations, the authors speculated that nucleation of α-Al_2O_3 from γ-Al_2O_3 was a cooperative athermal process. Shear transformations require an orientation relationship between the matrix and nucleating phases because of the need for a common 'habit' plane between the two phases. Again, however, the observation of an orientation relationship cannot be taken as definitive proof of a martensitic transformation.

A study by Zielinski *et al.* [35] on high energy ball milling of transition alumina powders also claims evidence for a shear nucleation mechanism. The high energy impacts resulted in complete conversion to α-Al_2O_3 at 'room temperature'. The authors reported that the γ-Al_2O_3 undergoes a certain degree of milling before α-Al_2O_3 nucleates, which they attribute to the time required for the γ-Al_2O_3 crystals to aggregate and form a 'mosaic' structure. The authors report a maximum γ-Al_2O_3 crystal size of ~5 nm and an initial α-Al_2O_3 crystal size of ~26 nm. Because shear mechanisms are enhanced by stress, the effect of the high energy ball milling appears to support the shear nucleation theory. Rapid movement of the dislocations through the θ-Al_2O_3 crystals, converting them to α-Al_2O_3, was suggested to occur even at low temperature in a manner similar to cold working in steels [30, 31].

The major evidence for the shear nucleation theory is that θ-Al_2O_3 crystals appear to coarsen to a critical size, as determined by XRD, TEM, and surface area measurements, before α-Al_2O_3 nucleates. The large, initial α-Al_2O_3 crystal sizes, which are generally twice as large as the crystals in the θ-Al_2O_3 matrix, lend support to the idea that large θ-Al_2O_3 crystals could shear to form large α-Al_2O_3 crystals, as discussed earlier in relation to Fig. 2a. Orientation relationships between the θ-Al_2O_3 and α-Al_2O_3 and the crystallography of the ccp to hcp transformation have also been used as suport, albeit inconclusive, for the mechanism.

2.2. Evidence for diffusional nucleation

Diffusional nucleation of α-Al_2O_3 has received little attention relative to the number of studies that contend that the process is martensitic. Most authors who support diffusional nucleation mention the mechanism only as a component of 'nucleation and growth' [27, 28]. As discussed earlier, a critical size of ~20 nm may be a prerequisite for diffusional nucleation if potent defects or surface sites needed to be formed. Nucleation of α-Al_2O_3 from the surface of transition alumina particles followed by growth of α-Al_2O_3 into the particle has been observed in sectioned transition alumina particles using TEM [36]. An important point is that surface nucleation is not conclusive proof of diffusional nucleation since shear transformations could also nucleate from the surface of crystals [29]. In addition, the nucleation and growth of the α-Al_2O_3 was observed in polycrystalline transition alumina particles rather than in a single crystal [36].

One major point supporting the diffusional nucleation of α-Al_2O_3 from θ-Al_2O_3 is the effect of seed particles. Many studies have shown that the addition of particles that are crystallographically isostructural with α-Al_2O_3 accelerates the transformation to α-Al_2O_3 by providing low energy sites for diffusional nucleation or growth [10–12, 16]. The incubation time for the transformation is also substantially reduced. McArdle and Messing [11] added large (~20 μm) α-Fe_2O_3 particles to θ-Al_2O_3 to observe the nucleation of α-Al_2O_3. TEM of the interface between the α-Al_2O_3 and α-Fe_2O_3 showed that heterogeneous (epitaxial) diffusional nucleation followed by diffusional growth was responsible for the accelerated transformation rates due to seeding [11]. McArdle and Messing also seeded 5 nm boehmite gels with 15–90 nm sized α-Fe_2O_3 crystallites and determined that the $\theta \rightarrow \alpha$ transformation was greatly enhanced at e.g., 1100°C (Fig. 3). The transformation curves for both seeded and unseeded samples were sigmoidal in character (Fig. 3) which is indicative of a diffusional phase transformation. In addition, the incubation time was reduced from approximately 100 minutes at 1100°C (unseeded sample) to 1 minute at 1100°C (seeded sample). The rate constant (k) was found to be 1×10^{-4} for the unseeded sample and 3.9×10^{-3} for the seeded sample. Assuming that:

$$k = C N_v G^n \qquad (2)$$

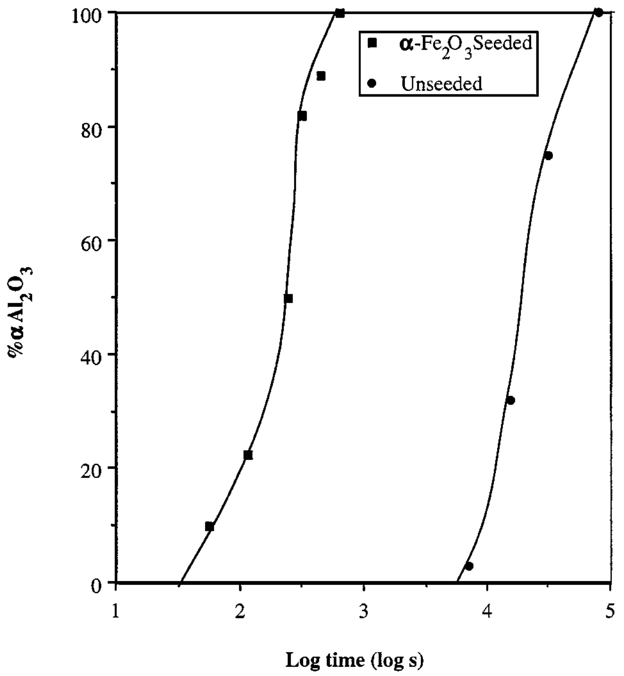

Figure 3 Effect of seeding on the $\theta \rightarrow \alpha$ transformation. (Data abstracted from McArdle and Messing [11]).

where C and n are constants, N_V is the nucleation density and G is the growth rate implies that the nucleation density is increased by a factor of approximately 40 for the seeded sample (assuming that the growth rate remains unaltered in the seeded and unseeded samples). Hence, the effect of the seeds can be attributed to the phenomenon of epitaxial nucleation of α-Al$_2$O$_3$ on α-Fe$_2$O$_3$. This increases the diffusional nucleation rate over that observed in the unseeded system where the preferred nucleation sites are likely to be free surfaces and grain boundaries.

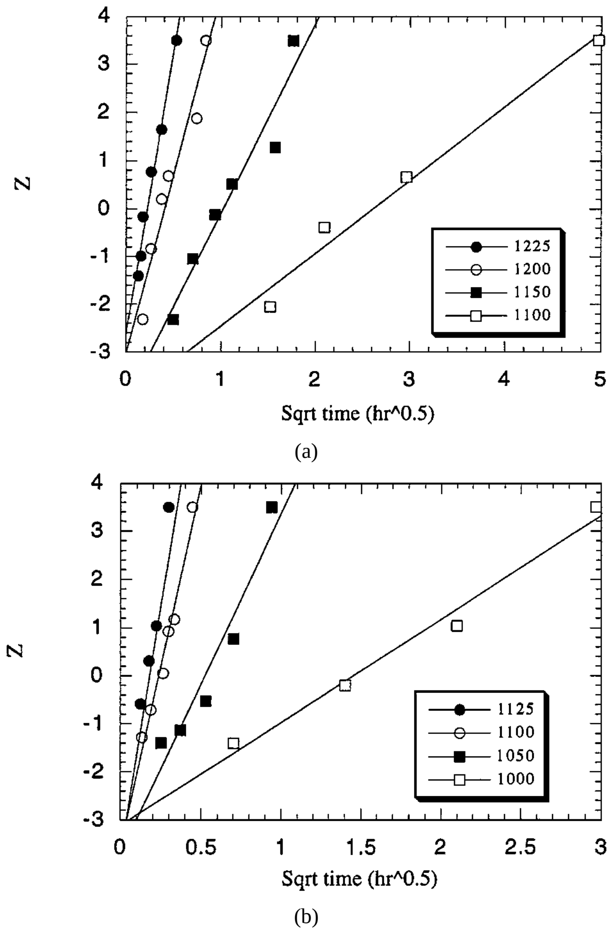

(a)

(b)

Figure 4 Transformation data of McArdle and Messing [11] analyzed by the synchro-shear model of Wynnyckyj and Morris [25]; (a) unseeded samples and (b) α-Fe$_2$O$_3$ seeded samples.

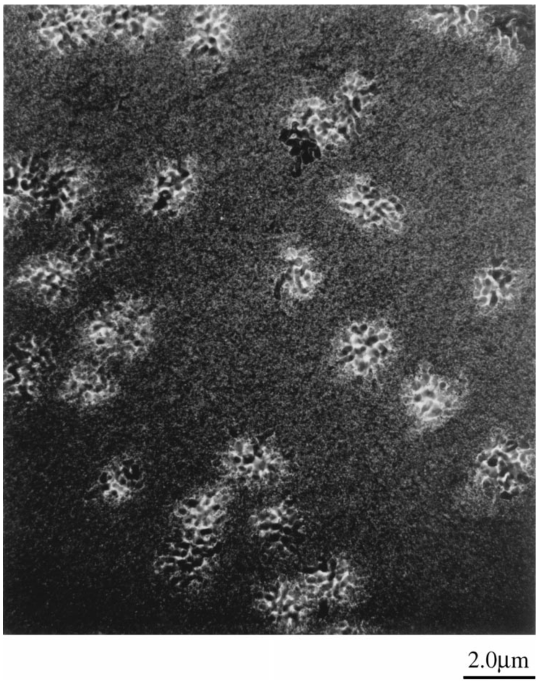

Figure 5 Bright field TEM image of unseeded pseudoboehmite thin film heated at 1100°C for 2 hours, showing nucleation and growth of α-Al$_2$O$_3$ colonies.

2.3. Interpretation of nucleation evidence

2.3.1. *Critical θ-Al$_2$O$_3$ crystal size*

The critical θ-Al$_2$O$_3$ crystal size is the most commonly reported evidence for shear nucleation and in many studies is the only evidence cited. The synchro-shear model of Wynnyckyj and Morris [25] relies primarily on the development of the θ-Al$_2$O$_3$ crystal size. The θ-Al$_2$O$_3$ to α-Al$_2$O$_3$ transformation data fit the synchro-shear model very well, but the success is for the most part due to the diffusional aspects of the model. For example, the transformation data of McArdle and Messing [11]* for unseeded and α-Fe$_2$O$_3$-seeded transition aluminas was entered into the synchro-shear model to test an 'intrinsically' nucleated system against an 'extrinsically' (seeded) nucleated system. The results of the analysis are shown in Fig. 4. The average correlation coefficient (r) for the set of transformation curves for the seeded samples (0.98) was nearly the same as for the unseeded samples (0.97). Seeding the transformation with α-Fe$_2$O$_3$ eliminates any need for shear-type nucleation (see above) and might have resulted in a very poor fit to the model of Wynnyckyj and Morris. The synchro-shear model apparently contradicts the observations of many studies [7, 16], demonstrated in Fig. 5, that nucleation of α-Al$_2$O$_3$, followed by rapid growth, occurs simultaneously throughout the

---

* These data show prototypical features of diffusional nucleation and growth transformations (and see Fig. 3).

transition alumina matrix. Growth of the vermicular α-Al_2O_3 colonies is then responsible for most of the transformation. The synchro-shear model assumes each θ-Al_2O_3 crystal coarsens to the critical size and then transforms martensitically to α-Al_2O_3.

In the study of Bye and Simpkin [8], the sole evidence for the shear mechanism is the observation that the surface area significantly decreases before α-Al_2O_3 nucleates. The results in the doped samples are particularly difficult to interpret in terms of the synchro-shear model because of the possibility of the formation of 'seeds' such as α-Fe_2O_3 that could provide epitaxial nucleation sites, as discussed earlier. Since impurities in a crystal can inhibit a shear transformation by resisting the cooperative motion of the atoms [29], a dopant such as Cr^{6+}, Cr^{3+}, or Fe^{3+} incorporated into the crystal structure should inhibit the transformation to α-Al_2O_3. The possibility that α-Fe_2O_3 'seeded' the transformation is indirect support for the diffusional nucleation mechanism.

The critical crystal size is insufficient evidence to support the shear nucleation model. The coarsening of the θ-Al_2O_3 crystals most likely is due to the incubation time required to produce α-Al_2O_3 nuclei. Recent studies [42, 43] report that γ-Al_2O_3 may be energetically and thermodynamically stable at surface areas greater than 125 m^2/g due to surface energy and adsorbed water effects, which would also lead to a critical degree of coarsening before nucleation of α-Al_2O_3. As shown in Fig. 6, the incubation time decreases with increasing temperature which is consistent with a diffusional nucleation (thermally activated) mechanism. The probable insignificance of the θ-Al_2O_3 crystal size is supported by the observation, shown in Fig. 7, that nucleation of α-Al_2O_3 occurs in a variety of different θ-Al_2O_3 crystal sizes and is noticeably absent from many 100 nm and larger θ-Al_2O_3 crystals. If a critical θ-Al_2O_3 crystal size was necessary, α-Al_2O_3 should nucleate more readily in larger θ-Al_2O_3 crystals. The wide range of critical θ-Al_2O_3 crystal sizes reported in the literature (Table I) can be explained by the observation that α-Al_2O_3 nucleation is not a consequence of the θ-Al_2O_3 crystal size, rather the wide range of crystal sizes are a reflection of the difficulty of diffusional nucleation.

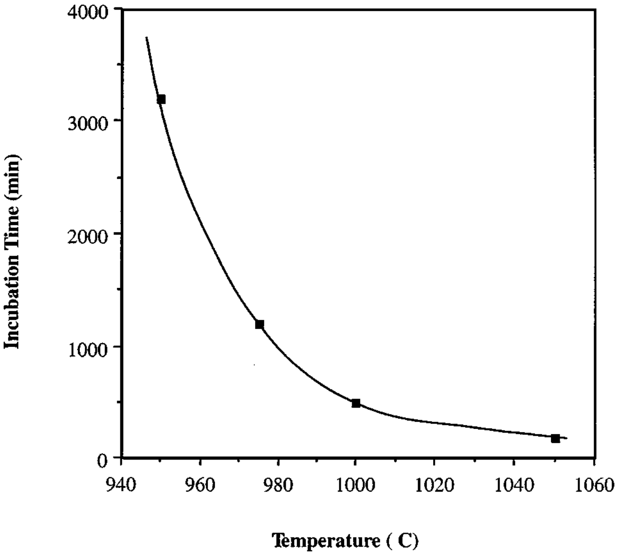

Figure 6 Incubation time for the formation of α-Al_2O_3 in pseudo-boehmite-derived θ-Al_2O_3 as a function of heating temperature.

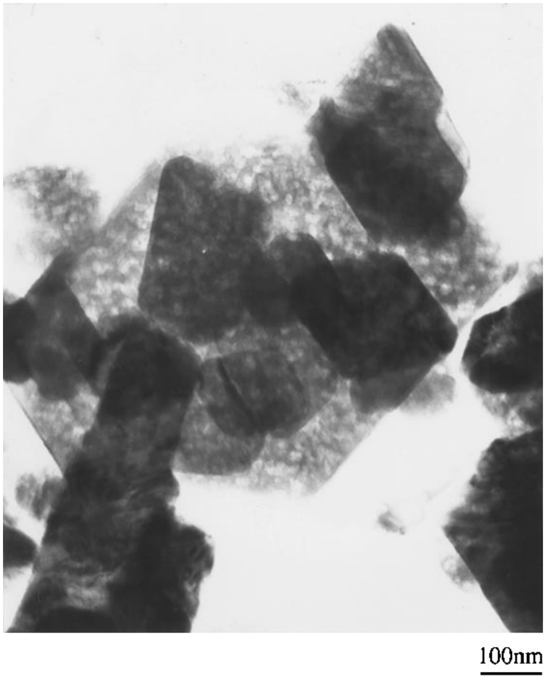

Figure 7 Bright field TEM image of θ-Al_2O_3 crystals formed from well crystallized boehmite heated at 1100°C for 5 hours.

2.3.2. Formation of large α-Al_2O_3 nuclei

The common observation that 100–1000 nm crystals of α-Al_2O_3 are initially formed, can be explained by the limited number of effective nucleation sites in the transition alumina matrix. The intrinsic nucleation density of α-Al_2O_3 colonies has been reported as 10^8–10^{10} nuclei/cm^3 in boehmite-derived transition aluminas [7, 16]. Choosing 10^{10} nuclei/cm^3 as the nucleation density and assuming each nucleation event produces one grain in the final microstructure allows the calculation of the α-Al_2O_3 crystal size at various degrees of transformation. Assuming that the α-Al_2O_3 nuclei are arranged in the corners of imaginary cubes, a nucleation density of $N_v = 10^{10}$ nuclei/cm^3 leads to an α-Al_2O_3 nuclei spacing (λ) of about:

$$\lambda = \frac{1}{N_v^{1/3}} = 4.6\ \mu m \tag{3}$$

In addition, to a first approximation and neglecting the overall ~20% decrease in specific volume during the transformation, the post transformation α-Al_2O_3 grain size (D) will also be 4.6 μm (i.e., $\lambda \cong D$).

Now, the lower detection limit of XRD is 2% transformation to α-Al_2O_3. Hence:

$$\frac{\pi D_{MIN}^3}{6} = 0.02\,(4.6)^3 \tag{4}$$

where D_{MIN} represents the minimum detectable α-Al_2O_3 diameter and:

$$D_{MIN} \cong 1.5\ \mu m \tag{5}$$

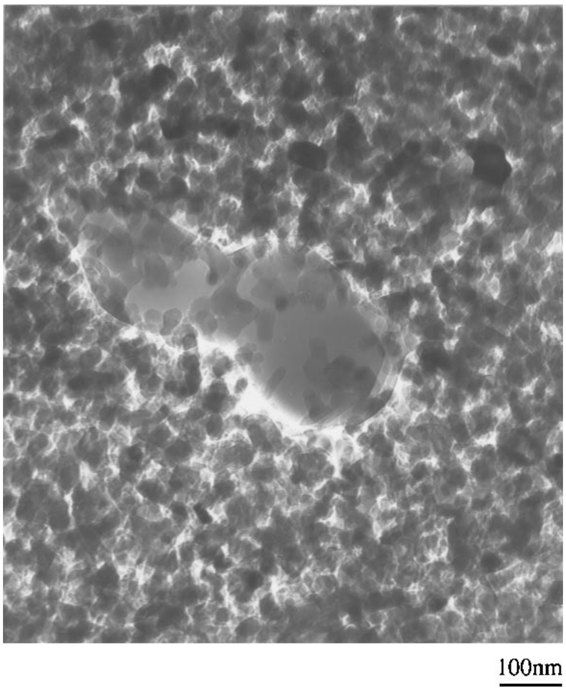

Figure 8 Pseudoboehmite thin film heated at 1100°C for 1 hour illustrating difficulty in detecting α-Al_2O_3 nuclei before they grow to $\sim$100 nm and larger.

The large initial α-Al_2O_3 crystal sizes reported in the literature therefore may simply be due to the inability to detect the α-Al_2O_3 crystals by XRD and other techniques before they reach a size that is much larger than the θ crystals in the transition alumina matrix. One important point illustrated by the calculation above is that systems where the nucleation density is less than $\sim 10^{12}$ nuclei/cm^3 will tend to form nuclei that appear very large when first detected by XRD. Similarly, it is difficult to observe α-Al_2O_3 nuclei in the TEM before they have grown considerably larger than the transition alumina matrix. Fig. 8 is a TEM micrograph illustrating the large discrepancy in the size of the θ-Al_2O_3 crystals and the smallest α-Al_2O_3 nuclei detected in a partially transformed pseudoboehmite film.

Equation 3 may also be used to examine the effect of seeding on the final transformed grain size by plotting log D as a function of log N (Fig. 9). Note that the α-Al_2O_3 grain size can be decreased from 4.6 μm for an unseeded sample ($N_v = 10^{10}$ cm^{-3}) to 0.2 μm for a seeded sample with $N_v = 10^{14}$ cm^{-3}. Although the above calculations are simplistic, they correlate remarkably well with recent studies by Nordahl [44].

Another factor contributing to the detection of large α-Al_2O_3 nuclei is the rapid consumption of θ-Al_2O_3 crystals after α-Al_2O_3 nucleation. This rapid growth, which is enhanced by the heat generated during the exothermic θ-Al_2O_3 to α-Al_2O_3 transformation, would also result in "abnormally large" initial α-Al_2O_3 crystal sizes. The rapid growth of crystals or grains during a massive phase transformation has been reported for alumina and in other systems such as the anatase to rutile transformation in titania [37].

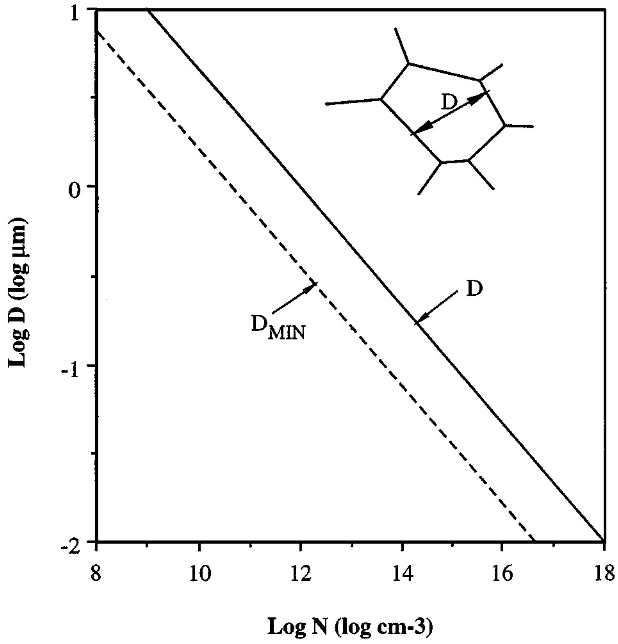

Figure 9 Plot of the post transformation α-Al_2O_3 grain size (D) and the minimum detectable α-Al_2O_3 grain size at 2% transformation (D_{MIN}) as a function of the nucleation frequency (N_v). For details: see text.

2.3.3. Orientation relationships

The observation of an orientation relationship is also not proof of a shear nucleation mechanism [41]. Diffusional nucleation also results in an orientation relationship to reduce the energy barrier to nucleation [30]. For example, in Cu-Si alloys, the similarity in the atomic spacings within the (111) fcc planes of the copper rich α phase and within the (0001) hcp planes of the silicon rich κ phase leads to the orientation relationship [30];

$$(111)\alpha//(0001)\kappa$$
$$[\bar{1}10]\alpha//[11\bar{2}0]\kappa$$

between the two phases. This orientation relationship, together with that documented by Kachi *et al.* [34], are frequently observed in fcc to hcp transformations (both diffusional and martensitic).

2.3.4. Further discrepancies in the shear nucleation model

In addition to the inconclusive nature of the evidence for shear nucleation, several key characteristics of shear transformations are not present in the θ-Al_2O_3 to α-Al_2O_3 transformation. For example, the shear nucleation of α-Al_2O_3 should result in a high defect concentration in the transformed α-Al_2O_3. Shear transformations commonly nucleate at defects such as groups of dislocations due to the lower energy barrier. Furthermore, stacking faults should result from the shear transformation of a ccp structure to hcp, as noted earlier. Bright and dark field imaging of the α-Al_2O_3 formed in both the pseudoboehmite (Fig. 8) and well crystallized boehmite (Figs 9 and 10) demonstrates that the only visible defects are the pores entrapped during the growth of α-Al_2O_3. The distinct morphology that is a result of the cooperative nature of shear transformations (i.e., a plate

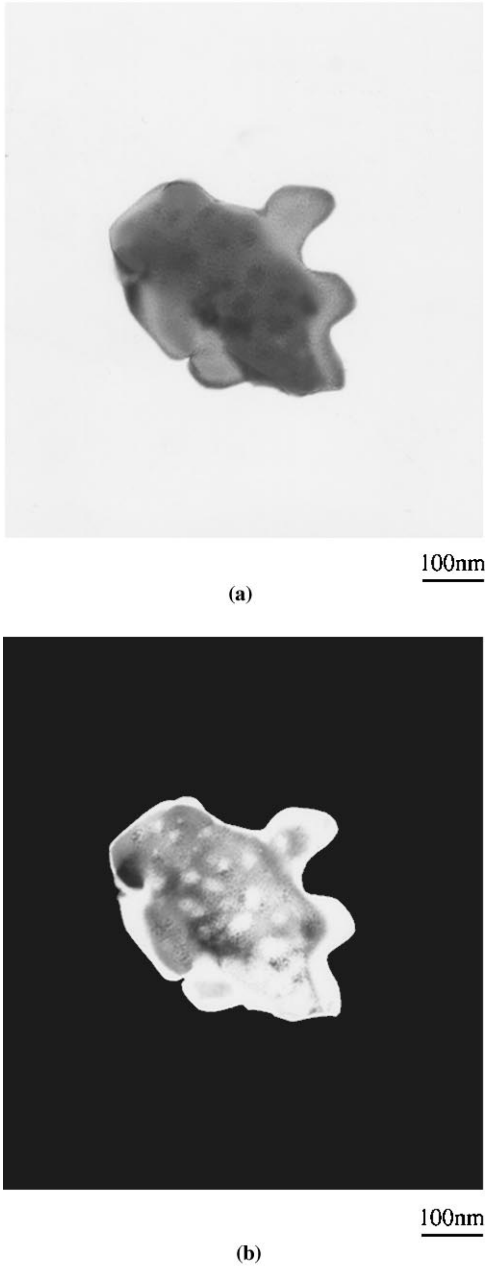

Figure 10 Two-beam bright field (a), and centered dark field (b) images of a single α-Al_2O_3 crystallite formed from well-crystallized boehmite heated at 1200°C for 15 minutes.

or a lath) is also not observed in the transformed crystals. A shear transformation requires the formation of a habit plane between the matrix and nucleating phases, as mentioned previously. The habit plane requirement results in a plate morphology similar to that observed in systems like zirconia and steels [29–33]. Based on the number of inconsistencies in the shear nucleation model, it is unlikely that the nucleation of α-Al_2O_3 occurs by shear of an entire θ-Al_2O_3 crystal that has reached a 'critical size'.

One study that is difficult to disregard as evidence for shear nucleation is the high energy ball milling study of Zielinski *et al.* [35]. However, high energy ball milling could enhance the transformation to α-Al_2O_3 through several processes that do not require shear nucleation. The impact energy being introduced into the transition alumina crystals could provide the driving force for the transformation to α-Al_2O_3, regardless of the nucleation mechanism. Many studies on high energy ball milling have demonstrated that a variety of materials such as lead oxide and calcium carbonate can be transformed to their stable form by the high energy impacts [38–40]. The local temperatures in high energy ball milling have also been estimated as 200–500°C higher than the entire milling system, which would provide greater diffusivities than at room temperature [39]. The impacts would also increase the number of potential surface and defect nucleation sites for any nucleation mechanism. Finally, the transformation from θ-Al_2O_3 to α-Al_2O_3 involves a $\sim$10% decrease in volume, which would be favored by the application of pressure.

3. Concluding remarks

The nucleation of α-Al_2O_3 appears to occur by a classical diffusional mechanism that does not require the growth of the transition alumina crystals to a critical size. The critical θ-Al_2O_3 crystal size that is commonly observed in the nucleation of α-Al_2O_3 is a result of the incubation time required to produce α-Al_2O_3 nuclei. The extremely large α-Al_2O_3 nuclei that have been reported in the literature are not due to the shear of large θ-Al_2O_3 crystals, but are due to the difficulty in detecting small nuclei in a low nucleation density system and the rapid growth of the α-Al_2O_3 after nucleation.

Acknowledgements

This work was supported by a grant from 3M Company, St. Paul, MN.

References

1. E. DORRE and H. HUBNER, "Alumina; Processing, Properties, and Applications" (Springer-Verlag, 1984).
2. W. H. GITZEN, "Alumina as a Ceramic Material" (The American Ceramic Society, 1970).
3. K. WEFERS and C. MISRA, "Oxides and Hydroxides of Aluminum" (Alcoa Technical Paper No. 19, 1987).
4. R.-S. ZHOU and R. L. SNYDER, *Acta. Cryst.* **B47** (1991) 617.
5. R. K. ILER, *J. Amer. Ceram. Soc.* **44** (1961) 618.
6. B. C. LIPPENS and J. J. STEGGERDA, in "Physical and Chemical Aspects of Adsorbents and Catalysts," B. G. Linson (ed.) (Academic Press, London) 1970, p. 171.
7. F. W. DYNYS and J. W. HALLORAN, *J. Amer. Ceram. Soc.* **65** (1982) 442.
8. G. C. BYE and G. T. SIMPKIN, *ibid.* **57** (1974) 367.
9. L. PACH, R. ROY and S. KOMARNENI, *J. Mater. Res.* **5** (1990) 278.
10. M. KUMAGAI and G. L. MESSING, *J. Amer. Ceram. Soc.* **68** (1985) 500.
11. J. L. McARDLE and G. L. MESSING, *ibid.* **76** (1993) 214.
12. R. A. SHELLEMAN, G. L. MESSING and M. KUMAGAI, *J. Non-Cryst. Solids* **82** (1986) 277.
13. F. W. DYNYS and J. W. HALLORAN, in "Ultrastructure Processing of Ceramics, Glasses, and Composites," L. Hench and D. Ulrich (eds.) (J. Wiley and Sons, NY) 1984, p. 142.
14. X. YANG, A. C. PIERRE and D. R. UHLMANN, *J. Non-Cryst. Solids* **100** (1988) 371.
15. S. J. WILSON, J. D. C. McCONNELL and M. H. STACEY, *J. Mater. Sci.* **15** (1980) 3081.
16. W. A. YARBROUGH and R. ROY, *ibid.* **2** (1987) 494.
17. R. F. WATERS, J. B. PERI, G. S. JOHN and H. S. SEELIG, *Ind. Eng. Chem.* **52** (1960) 415.
18. H. YANAGIDA, G. YAMAGUCHI and J. KUBOTA, *J. Ceram. Assoc. Jap.* **74** (1966) 371.

19. E. KATO, K. DAIMON and M. NANBU, *J. Amer. Ceram. Soc.* **64** (1981) 436.
20. J. L. HENRY and H. J. KELLY, *ibid.* **48** (1965) 217.
21. G. CARTURAN, R. DI MAGGIO, M. MONTAGNA, O. PILLA and P. SCARDI, *J. Mater. Sci.* **25** (1990) 2705.
22. V. N. KUKLINA, E. A. LEVITSKII, L. M. PLYASOVA and V. I. ZHARKOV, *Kinetika i Kataliz* **13** (1972) 1269.
23. V. N. KUKLINA, L. M. PLYASOVA, L. M. KEFELI and E. A. LEVITSKII, *ibid.* **12** (1971) 1078.
24. K. HAYASHI, S. TOYODA, H. TAKEBE and K. MORINAGA, *J. Ceram. Soc. Japan, International Edition* **99** (1991) 535.
25. J. R. WYNNYCKYJ and C. G. MORRIS, *Met. Trans. B.* **16B** (1985) 345.
26. T. C. CHOU and T. G. NIEH, *J. Amer. Ceram. Soc.* **74** (1991) 2270.
27. P. A. BADKAR and J. E. BAILEY, *J. Mater. Sci.* **11** (1976) 1794.
28. J. BERETKA and M. J. RIDGE, *J. Chem. Soc. A* (1967) 2106.
29. Z. NISHIYAMA, "Martensitic Transformation" (Academic Press, 1978).
30. D. A. PORTER and K. E. EASTERLING, "Phase Transformations in Metals and Alloys" (Chapman and Hall, 1981).
31. R. W. HERTZBERG, "Deformation and Fracture Mechanics of Engineering Materials" (John Wiley and Sons, 1989).
32. A. H. HEUER, N. CLAUSSEN, W. M. KRIVEN and M. RUHLE, *J. Amer. Ceram. Soc.* **65** (1982) 642.
33. A. H. HEUER and M. RUHLE, *Acta Metall.* **33** (1985) 2101.
34. S. KACHI, K. MOMIYAMA and S. SHIMIZU, *J. Phys. Soc. Japan* **18** (1963) 106.
35. P. A. ZIELINSKI, R. SCHULZ, S. KALIAGUINE and A. VAN NESTE, *J. Mater. Res.* **8** (1993) 2985.
36. D. S. TUCKER, *J. Amer. Ceram. Soc.* **68** (1985) C163.
37. K. N. P. KUMAR, *Scripta Met. et Mat.* **32** (1995) 873.
38. I. J. LIN, S. NADIV and D. J. M. GRODZIAN, *Minerals Sci. Engng* **7** (1975) 313.
39. R. M. DAVIS, B. McDERMOTT and C. C. KOCH, *Met. Trans. A.* **19A** (1988) 2867.
40. I. J. LIN and S. NADIV, *Mat. Sci. Eng.* **39** (1979) 193.
41. F. K. LeGOUES, K. CHATTOPADHYAY and H. I. AARONSON, *Scrupta Met.* **17** (1983) 675.
42. J. M. McHALE, A. NAVROTSKY and A. J. PERROTTA, *J. Phys. Chem.* **101** (1997) 603.
43. J. M. McHALE, A. AUROUX, A. J. PERROTTA and A. NAVROTSKY, *Nature.* **277** (1997) 788.
44. C. S. NORDAHL, Ph.D. thesis, The Pennsylvania State University, 1997.

Received 25 February
and accepted 16 August 1999